Modeling Reservoir Geometry With Irregular Grids

Z.E. Heinemann, SPE, **C.W. Brand, Margit Munka,** SPE, and **Y.M. Chen,** Mining U. of Leoben

Summary. This paper describes a practical method in which irregular or locally irregular grids are used in reservoir simulation with the advantages of flexible approximation of reservoir geometry and reduced grid-orientation effects. Finite-difference equations are derived from an integral formulation of the reservoir model equations equivalent to the commonly used differential equations. Integrating over gridblocks results in material-balance equations for each block. This leads to a finite-volume method that combines the advantages of finite-element methods (flexible grids) with those of finite-difference methods (intuitive interpretation of flow terms). Grid-orientation effects are investigated. For grids based on triangular elements, the more isotropic distribution of gridpoints diminishes the orientation effect significantly. Numerical examples show that the regions of interest in a reservoir can be simulated efficiently and that well flow can be represented accurately.

Introduction

The accurate and efficient simulation of complex reservoirs depends highly on proper grid selection. Grids based on a Cartesian coordinate system have been widely used, but have some disadvantages: (1) inflexibility in description of faults, pinchouts, and discontinuities of reservoir parameters; (2) inflexibility in representation of well locations; and (3) the influence of grid orientation on the results.

Local grid refinement[1-6] and nine-point difference schemes[7,8] were introduced to improve the performance of the Cartesian grid technique.

To diminish grid-orientation effects, Pruess and Bodvarsson[9] presented a uniform hexagonal gridblock pattern. Grids based on orthogonal curvilinear coordinate systems were proposed by Hirasaki and O'Dell[10] and investigated by Sonier and Chaumet,[11] Robertson and Woo,[12] and Fleming.[13] Curvilinear coordinate systems, defined by streamlines and equipotential lines, can be more appropriate for the flow pattern under consideration. If the coordinate system is not strictly orthogonal, however, mixed derivative terms have to be introduced that distort the structure of the linear equation. For this reason, the mixed derivatives were usually neglected. The finite-difference approximation based on such nonorthogonal grids, sometimes called corner-point geometry, can result in considerable errors and is not applicable for simulation.

In this paper, irregular gridblock systems for simulation of complicated reservoirs are proposed. The multiphase flow equations are discretized with a finite-volume approach. Anisotropic permeability is taken into account. Gridblock systems based on perpendicular bisectors are described, and grid-orientation effects are examined. The performance of these irregular grids is demonstrated by numerical examples (a single-phase, a black-oil, and a steam-drive simulation).

Finite-Volume Discretization

An integral approach similar to that described by Nghiem[14] and Pedrosa and Aziz[15] is applied to discretize the multiphase flow equations. The conservation of mass within a control volume V is expressed for the component k as a balance between the accumulation within V and the flow through its surface A:

$$-\int_A \left(\sum_{p=1}^{n_p} \vec{u}_p \xi_p x_{pk} \right) \vec{n} \, dA + q_k = \frac{\partial}{\partial t} \int_V \left(\phi \sum_{p=1}^{n_p} S_p \xi_p x_{pk} \right) dV. \quad \ldots\ldots\ldots\ldots\ldots\ldots\ldots\ldots\ldots\ldots (1)$$

The phase velocity is given by the multiphase formulation of Darcy's law,

$$\vec{u}_p = -\lambda_p \bar{\bar{k}} \nabla \Phi_p. \quad \ldots\ldots\ldots\ldots\ldots\ldots\ldots\ldots\ldots\ldots\ldots\ldots\ldots\ldots (2)$$

Discretization of the conservation Eq. 1 involves two main steps: construction of an appropriate gridblock system and setup of proper difference equations for each gridblock.

Because Eq. 1 holds for volumes of arbitrary shape, some flexibility in constructing gridblocks is possible. The derivation of difference equations for blocks such as those presented in this paper lies, in some sense, midway between the finite-difference and finite-element approaches. This method offers the advantage of flexible approximation of the reservoir geometry by regular or irregular grids. In particular, the blocks used in the examples in this paper are based on triangular elements commonly used in finite-element methods. On the other hand, the method preserves the simple derivation and handling of finite-difference approximations, the local and illustrative modeling of flow in the neighborhood of a gridpoint, and the universality of finite differences with respect to various types of differential equations.

The method is called a finite-volume or -balance method or also a control-volume or integrated-finite-difference method. As these various names indicate, such methods have been used in many formulations (see Refs. 16 through 18 and the references cited therein). In fact, such an approach is used (at least implicitly) when the conventional conservative finite-difference equations for a Cartesian gridblock system are derived. Nevertheless, the freedom and flexibility in choosing the shape of the gridblocks apparently have not been exploited extensively in practical reservoir simulation examples thus far.

A gridblock system, as described here, consists of gridpoints and blocks surrounding each point. The blocks cover the whole reservoir region without leaving gaps or overlapping each other. For a given gridblock, the spatial discretization of the accumulation term is obtained by approximating the volume integral in Eq. 1 by a simple one-point quadrature formula:

$$\int_{V_I} (S_p \xi_p x_{pk}) dV = (S_p \xi_p x_{pk})_I V_I, \quad \ldots\ldots\ldots\ldots\ldots\ldots\ldots\ldots\ldots\ldots (3)$$

where $(S_p \xi_p x_{pk})_I$ is the average value of $S_p \xi_p x_{pk}$ over V_I, the volume of Gridblock I. For the time derivative, a first-order finite difference is used. The particular shape of the control volume V_I does not enter the difference expressions but essentially determines the form of the flow terms, which we explain in greater detail now.

Flow Terms. Surface A of a gridblock is partitioned into subsurfaces. Subsurface A_{IJ} is the part of A that is shared by Block I and neighboring Block J. Substituting Darcy's law (Eq. 2) into Eq. 1 and splitting the integral into a sum of integrals over subsurfaces allows the flow of the kth component from Block I to J to be written as

$$Q_{IJk} = \int_{A_{IJ}} \left[\sum_{p=1}^{n_p} \Lambda_{pk} (\bar{\bar{k}} \nabla \Phi_p) \right] \vec{n} \, dA. \quad \ldots\ldots\ldots\ldots\ldots\ldots\ldots\ldots\ldots\ldots (4)$$

To derive a finite-different expression, one has to approximate the surface A_{IJ}, the value of the scalar product $(\bar{\bar{k}} \nabla \Phi_p) \cdot \vec{n}$, and the component mobility Λ_{pk} on the surface A_{IJ}. The block volume V_I,

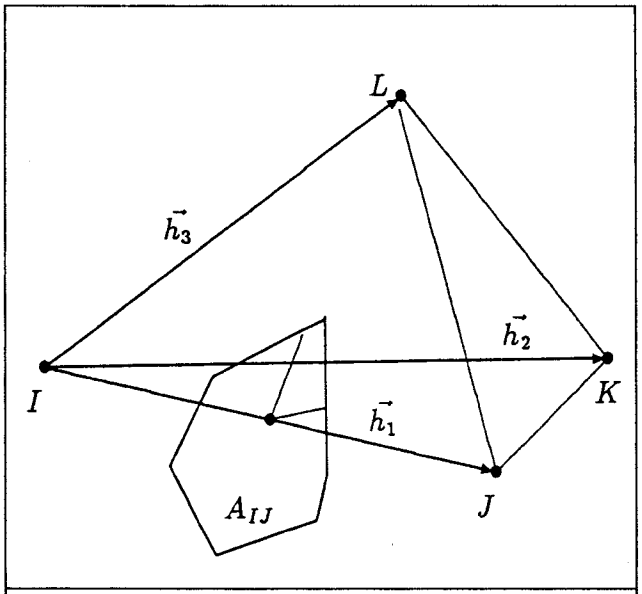

Fig. 1—Tetrahedron element to compute $\nabla\Phi$. Surface A_{IJ} connecting Blocks I and J and the segment of A_{IJ} intersecting the tetrahedron are shown.

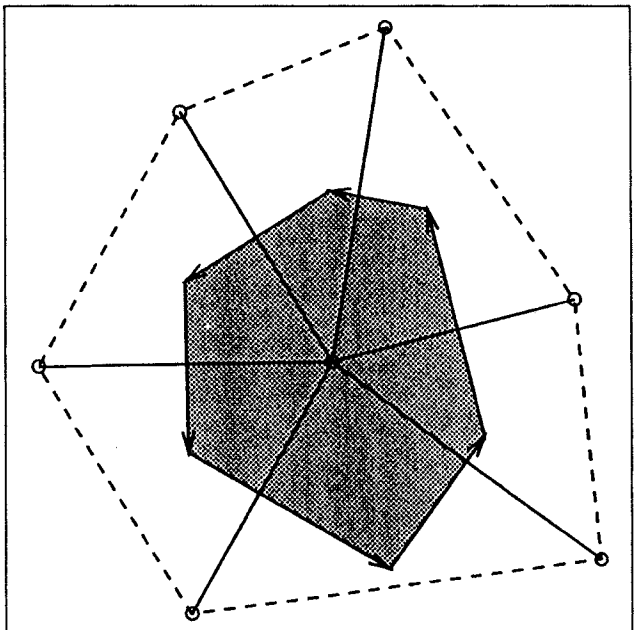

Fig. 2—Gridblock construction with perpendicular bisectors.

the surfaces A_{IJ}, and the orientation of the normal vector $\vec{n}_{IJ}$ are purely geometric properties of the gridblock system and are computed exactly during a numerical grid-generation procedure.

For Λ_{pk}, upstream mobility weighting is used: i.e.,

$$(\Lambda_{pk})_{A_{IJ}} = \begin{cases} \Lambda_{pkI} & \text{if } (\bar{\bar{k}}\nabla\Phi_p)\cdot\vec{n} > 0 \\ \Lambda_{pkJ} & < 0 \end{cases} . \quad \ldots\ldots\ldots\ldots\ldots\ldots\ldots\ldots\ldots\ldots (5)$$

To approximate all components of the vector $\nabla\Phi$ (subscript p is suppressed for convenience), at least four gridpoints, I, J, K, and L, are necessary in three dimensions. Assuming a linear variation of Φ within the tetrahedron defined by these points (**Fig. 1**) an expression for $\nabla\Phi$ (which is constant) can be derived and the dot product $\nabla\Phi\cdot\vec{n}$ can be computed. This approximation is used for the part of Surface A_{IJ} that intersects the tetrahedron element. See the Appendix for details.

Such an approach is closely related to finite-element Galerkin methods based on linear basis functions on triangular or tetrahedron elements. This relationship allows us to use the convergence statements for Galerkin methods to prove the convergence of the finite-volume discretization (at least in the single-phase limit). A thorough investigation on the convergence behavior is given by Heinrichs.[19]

Because (for an arbitrarily oriented A_{IJ}) all components of $\nabla\Phi$ generally have to be computed, not only the potential values at Gridpoints I and J enter the term Q_{IJk} representing flow between blocks I and J. In the following cases, however, the approximation can be simplified so that it fits the intuitive concept of evaluating flow through A_{IJ} by a transmissibility term times one potential difference $(\Phi_J-\Phi_I)$. We will deal with isotropic media first; i.e., the tensor $\bar{\bar{k}}$ can be replaced by scalar value k. The case of anisotropic media is treated in the Appendix.

Case 1. A_{IJ} is the perpendicular bisector of the straight line connecting Points I and J. Then,

$$k\nabla\Phi\cdot\vec{n}=(k/h_{IJ})(\Phi_J-\Phi_I). \quad \ldots\ldots\ldots\ldots\ldots\ldots\ldots\ldots\ldots\ldots (6)$$

A gridblock system based on an orthogonal curvilinear coordinate system would have this property, as would more general grids based on perpendicular bisectors. Such grids are described in the next section.

Case 2. Gridpoints I and J lie on the same streamline. Then $\nabla\Phi$ already points in the direction of $\vec{h}_{IJ}$, and the dot product is given by

$$k\nabla\Phi\cdot\vec{n}=(k/h_{IJ})(\Phi_J-\Phi_I)\cos\gamma, \quad \ldots\ldots\ldots\ldots\ldots\ldots\ldots\ldots\ldots\ldots (7)$$

where γ = angle between A_{IJ} and the streamline direction. This is called a streamtube grid.

While in Case 1 the orthogonality of A_{IJ} to the direction $\vec{h}_{IJ}$ is a purely geometric property of the grid, Case 2 is based on hydrodynamic assumptions that may be valid only in certain instances.

The discretization of the flow term given by Eq. 4 in the orthogonal or streamtube cases, respectively, can be written as

$$Q_{IJk}=\sum_{p=1}^{n_p}(\Lambda_{pk}k)_{IJ}b_{IJ}(\Phi_J-\Phi_I)_p, \quad \ldots\ldots\ldots\ldots\ldots\ldots\ldots\ldots\ldots\ldots (8)$$

where $b_{IJ}=A_{IJ}/h_{IJ}$ (orthogonal) or $A_{IJ}/h_{IJ}\cos\gamma$ (streamtube). Finally, one has to sum the flow terms over all neighbors $J=1\ldots n_J$. The complete discrete form of Eq. 1 is

$$-\sum_{p=1}^{n_p}Q_{IJk}^{n+1}+q_{Ik}^{n+1}V_I$$

$$=\frac{V_I\phi}{\Delta t}\sum_{p=1}^{n_p}[(S_p\xi_p x_{pk})_I^{n+1}-(S_p\xi_p x_{pk})_I^n]. \quad \ldots\ldots\ldots\ldots\ldots\ldots\ldots\ldots\ldots\ldots (9)$$

Grid Construction

The control-volume method allows us to derive difference equations on general grid systems. The gridpoints may form a network of triangles or quadrangles, or they may be selected on the basis of radial or other curvilinear coordinate systems. Discretization on a perpendicular bisection (PEBI) is a special case of the control-volume method where the flow terms are similar to standard finite-difference equations.

Construction of a 2D PEBI grid starts with defining the position of gridpoints and connecting them by straight lines so that a triangular mesh is formed. The triangular elements cover the whole reservoir region but do not intersect or overlap. Such triangulations are common in finite-element applications. A perpendicular bisection block system can be constructed from this mesh when the following additional regularity conditions are fulfilled: (1) for any two adjacent triangles, the sum of the two angles at the vertices opposite the common edge of the two triangles must not exceed π and (2) for a triangle at the boundary, the angle at the vertex opposite the boundary must not exceed $\pi/2$. A triangulation that satisfies these conditions is known as a Delauney triangulation.

For Gridpoint I in this triangulation, all Points $J=1\ldots n_J$ that are connected to Point I by the edge of a triangle are considered

neighbors. The gridblock corresponding to this point is defined as the region enclosed by all perpendicular bisectors of the edges joining Point I with its neighbors. The corners of this block are the circumcenters of all triangles having I as a corner point (**Fig. 2**). As long as a Delauney triangulation is considered, gridblocks constructed in this way will not overlap.

The procedure can be applied in three dimensions as well. Instead of triangles, tetrahedrons have to be considered. This gridblock resulting from the perpendicular bisection procedure also is called the Wigner-Seitz cell.

The grids used in the examples in this paper are PEBI grids in the areal dimensions. The gridpoints were projected vertically onto all layers of the reservoir, and a streamtube approach was used in the cross section (**Fig. 3**). This approach is practical for thin-layered reservoirs where the vertical extension is smaller than the horizontal one by an order of magnitude. The construction of an irregular gridblock system for a reservoir is feasible only if it is done by a numerical grid-generation procedure (see Ref. 20). The grids in the examples in this paper were constructed by a procedure consisting of the following steps.

1. The reservoir is covered with a mesh of equilateral triangles.
2. Near the boundary, mesh points of this regular mesh are projected onto the boundary or shifted toward the corners of the region. At well locations, the nearest point in the regular mesh is shifted at the position of the well. Through this step, the regularity of the mesh is distorted near boundaries and along wells.
3. Weighting factors are assigned to the points. In regions where a dense refinement is wanted, greater weighting factors are selected.
4. An iterative smoothing procedure is applied. The coordinates of each interior point (except well points) are replaced by a weighted mean of the coordinates of all neighboring points. By this procedure, the mesh converges to a triangulation in which the weighted sum of the squares of the edge lengths is minimized.
5. During the smoothing and refinement process, the angle restrictions of the Delauney triangulation may be violated. This is checked and corrected by changing some triangles or by removing points.
6. Having completed a correct triangulation, gridblocks are constructed by perpendicular bisection. Block volumes and interface areas are computed and provided as input for a reservoir simulator.

Numerical Results

Grid-Orientation Effects. Grid-orientation effects in reservoir simulation caused by five-point discretization were demonstrated by Todd *et al.*[21] Yanosik and McCracken[7] reported results for five- and nine-point Cartesian grids. As reported in a series of papers,[22-26] examination of these results indicates that the five-point predictions are erroneous. Here, these examples are used to compare the grid-orientation effect on five- and nine-point Cartesian and PEBI grids. The different orientations of the PEBI grids are shown in **Fig. 4. Fig. 5** compares the PEBI with the Cartesian grids.

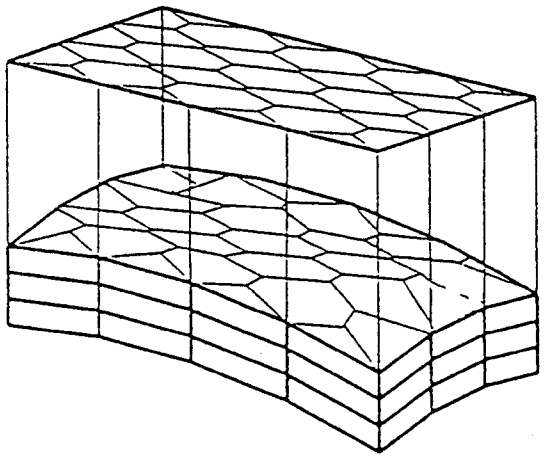

Fig. 3—3D PEBI grid model for reservoir simulation.

The nine-point Cartesian grid diminishes the orientation effect but does not eliminate it completely. The same is true for the PEBI grid, as becomes evident when the viscosity ratio (or mobility ratio) is increased to 50. As **Fig. 6** shows, the results are neither worse nor better than the comparable Cartesian results of Yanosik and McCracken.[7]

To get a more convincing comparison between the nine-point Cartesian and PEBI diagonal grids, the same example was computed with a straight-line relative permeability. The nine-point grid provides unrealistic results (**Fig. 7**). The saturation front does not move preferentially along the diagonal line connecting the injector and the producer. Consequently, a horned displacement front is formed. The PEBI grid shows a more realistic result.

In conclusion, the PEBI grid has as good (or better) performance with respect to the grid-orientation effect as the nine-point grid. This applies up to at least $M=50$.

Computational Efficiency. In reservoir simulation, we intend to describe accurately those regions of the reservoir where the pressure gradient is expected to change rapidly; for example, in the vicinity of a well. Grid refinement around wells is necessary for accurate resolution. A black-oil model is used as an example: a hypothetical six-layer reservoir that is 4200×4200×178 m [13,780×13,780×584 ft], with a gas cap and bottomwater. A locally refined Cartesian block model (**Fig. 8**) consisting of 2,256 blocks was selected to compare with an irregular PEBI grid model with 1,626 blocks (**Fig. 9**). The reservoir and production data (specified in Ref. 27) are the same for the two models.

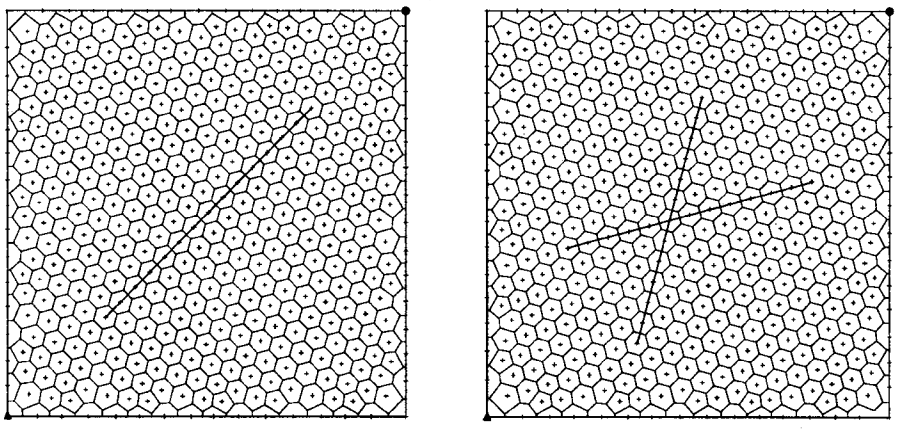

Fig. 4—Equivalent parallel and diagonal PEBI grids.

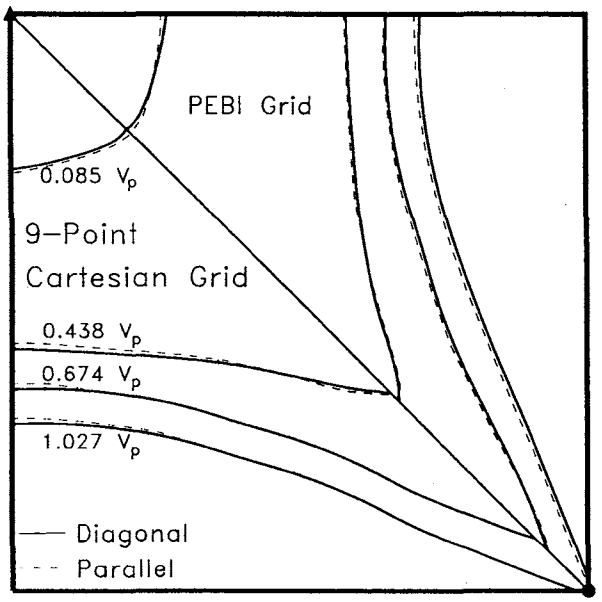

Fig. 5—Comparison of the displacement fronts ($S_d = 0.9$) of PEBI and Cartesian grids for $M = 10$ ($f_d = S_d^2$).

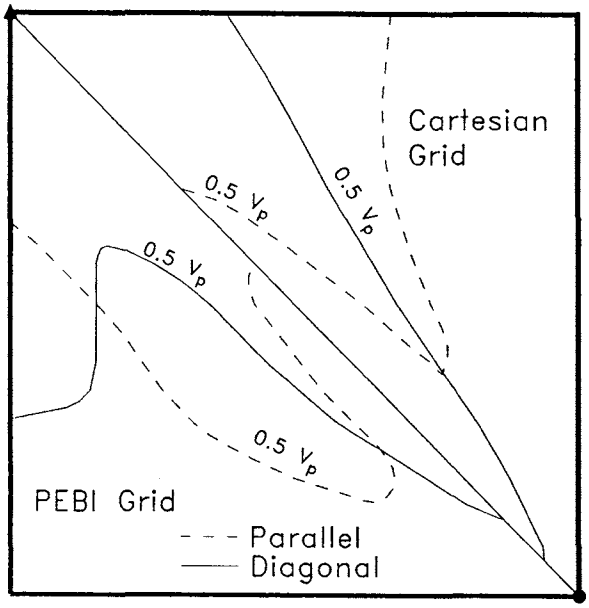

Fig. 6—Comparison of the displacement fronts ($S_d = 0.9$) of PEBI and Cartesian grids for $M = 50$ ($f_d = S_d^2$).

The PV of the wellblocks and the surrounding blocks is kept approximately equal in both grid models. **Table 1** gives a comparison of relative CPU time for both calculations. The example presents a PEBI grid as an alternative to locally refined Cartesian grids. The smooth change in block size, a feature of the PEBI grid, offers more flexibility and is more favorable with respect to discretization errors than a sharp interface between the fine and coarse grids. Therefore, the total number of blocks is lower than in the Cartesian example. Note that the CPU time per gridblock is approximately the same in both cases; i.e., the simulator can handle blocks in an irregular grid as well as locally refined Cartesian grids.

Fig. 10 shows a fairly good agreement in cumulative gas production. All other results were virtually identical (within the resolution of the plotter). The results of the PEBI grid are certainly reliable because this type of grid can model the radial flow around the wells better than the Cartesian grid, as demonstrated in the next example.

Well Representation. In this section, we show that the PEBI grid gives a good representation of the radial-flow performance around wells. The problem selected is the same as that used by Pedrosa and Aziz[15]: a well producing at a constant rate in the center of a square reservoir with one boundary at constant pressure and no-flow boundaries on the other three sides. The analytical solution for this problem in terms of the dimensionless time is given by Ramey *et al.*[28] Pedrosa and Aziz obtained a perfect match to the analytical solution by using a Cartesian/radial hybrid grid with a finer Cartesian grid in the reservoir region. Therefore, this example provides a comparison not only with the exact analytical solution, but also with a Cartesian/radial hybrid grid.

Fig. 11 shows the selected PEBI grid. The wellbore pressure is calculated with

$$p_{wf} = \bar{p} + 138.46(q\mu B/hk)[\ln(r_e/r_w) - c]. \quad \ldots\ldots\ldots\ldots (10)$$

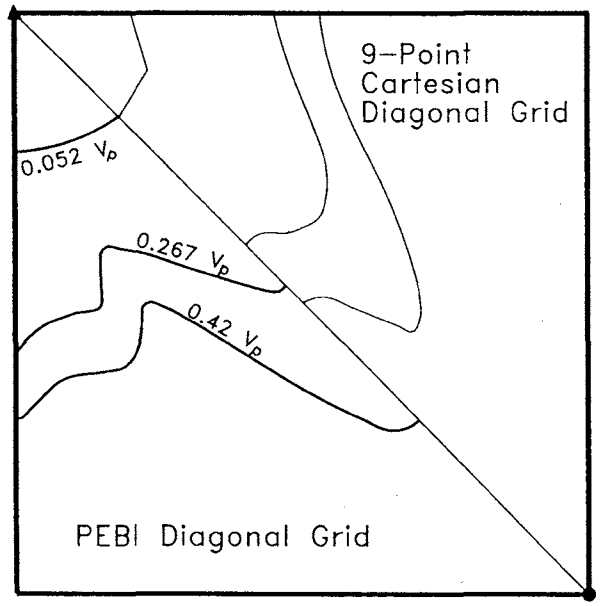

Fig. 7—Comparison of the displacement fronts ($S_d = 0.9$) of PEBI and Cartesian grids for $M = 10$ (straight-line k_{rd}).

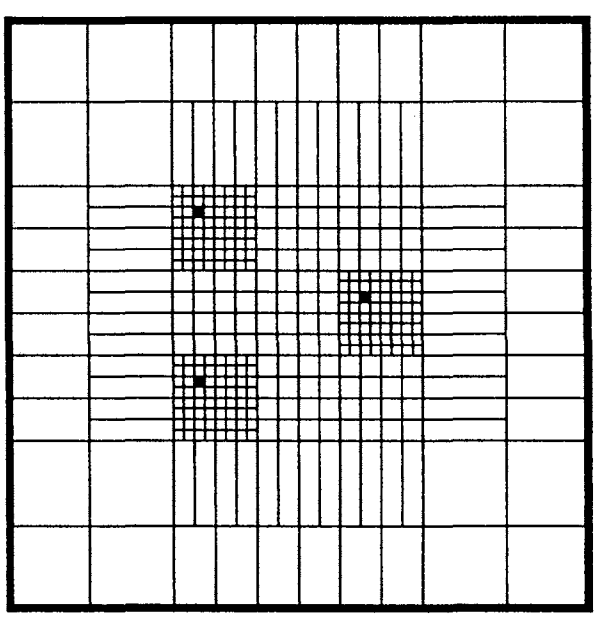

Fig. 8—Strongly refined Cartesian block model.

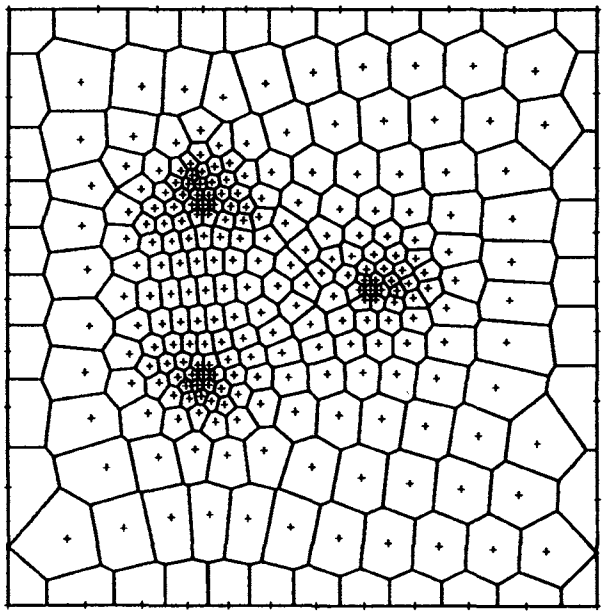

Fig. 9—PEBI block model.

TABLE 1—COMPARISON OF CPU TIME				
Grid	Steps	Repetitions	Iterations	Relative CPU Time
Cartesian	12	3	16	1.3
PEBI	12	3	16	1.0

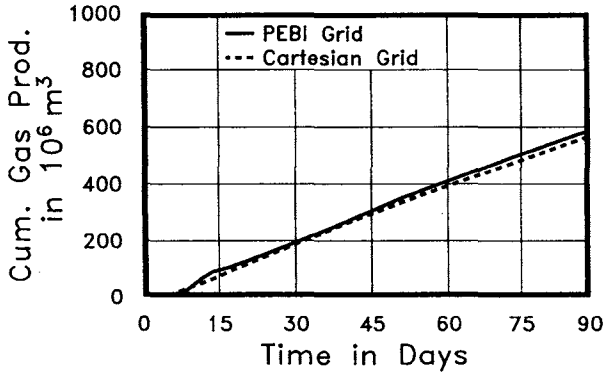

Fig. 10—Comparison of PEBI and Cartesian grids, cumulative gas production.

The values of the constant c and the effective radius, r_e, depend on the flow conditions and block geometry. Here, values for hexagonal blocks and stationary flow were used, $c=1.1$ and $r_e=\sqrt{A/\pi}$, where A=area of the basal surface of the wellblock.

Fig. 12 compares the analytical and numerical solutions. The numerical solution matches the analytical solution perfectly.

Simulation of Steamdrive. Flow-pattern simulation often is needed for better understanding and for feasibility studies of EOR processes. These models form a special class of grids. On one hand, it is easier to use special solutions because of the fixed geometry and homogeneous reservoir; on the other hand, expectations regarding reliability and accuracy are higher. These problems are classic examples for orthogonal curvilinear grids.

In the Fourth SPE Comparative Solution Project,[29] steam-injection simulators were compared for three problems. The second one is a steam displacement in an inverted nine-point pattern with a nonvolatile oil. This problem was calculated with the given Cartesian SPE grid using a nine-point difference scheme and an irregular grid. The calculation was made with the multipurpose simulator SURE and only one hydrocarbon component.

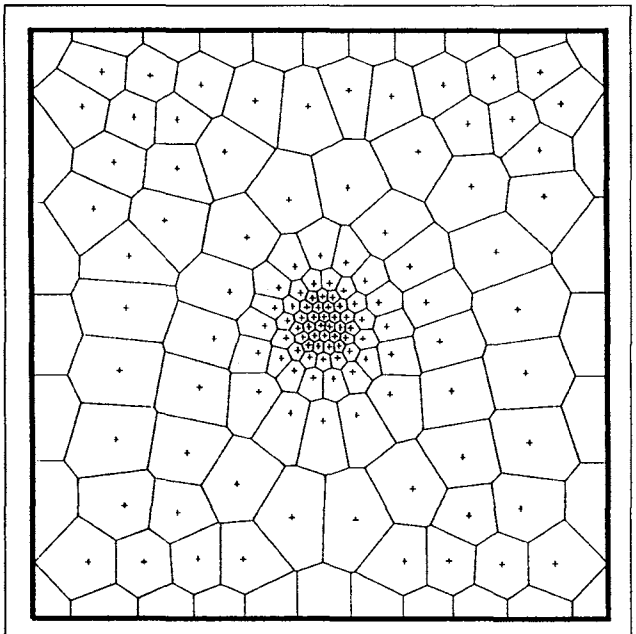

Fig. 11—Irregular grid for single-phase problem.

Fig. 13 shows the gridblock system. To get comparable results with the SPE grid, no refinement was done around the wells. The number of gridpoints is virtually the same (26 and 27) in both cases.

The results are presented in **Table 2** and **Fig. 14.** It can be concluded that the irregular PEBI grid gives comparable results with the nine-point Cartesian grid and can be used for flood patterns in a very flexible way. The advantage of the irregular grid in this case is not the higher accuracy but its flexibility. If necessary, more gridpoints can be used in the vicinity of the wells.

Conclusions

1. The PEBI grid has a high flexibility to represent the reservoir geometry, because the location of gridpoints can be chosen freely.
2. PEBI grids can be constructed so that they are dense around wells and have a smooth transition zone to the coarse-grid region. Such grids are very suitable for calculating radial flow and well performance.
3. The grid-orientation effect when a PEBI grid is used is lower than that when a five-point Cartesian grid is used and slightly higher than when a nine-point scheme is used.

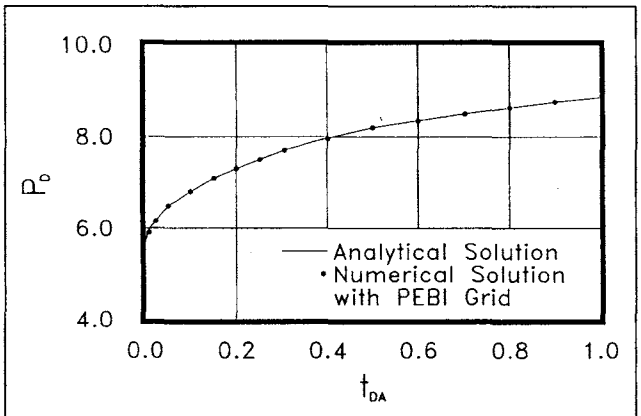

Fig. 12—Comparing the result of the PEBI grid with the analytical solution, single-phase problem.

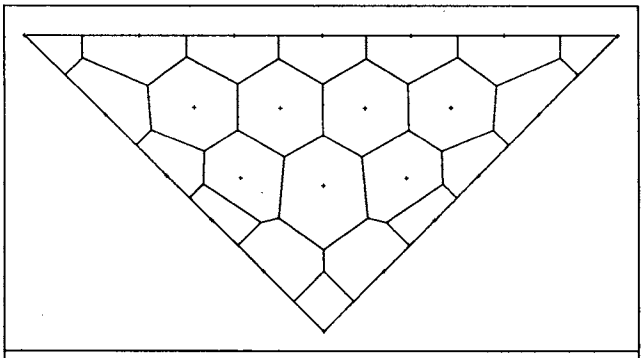

Fig. 13—PEBI gridblock system for the Fourth SPE Comparative Solution Project[29] nine-spot symmetry element.

TABLE 2—TIME FOR 10 STB/D OF STEAM RATE FOR PROBLEM 2a OF REF. 29

	Near Producer (days)	Far Producer (days)
Arco	336	2,245
Chevron	411	1,543
CMG	539	1,398
Mobil	257	1,583
SNEA	381	1,454
SSI	487	1,497
SURE Cartesian	330	1,379
SURE PEBI	360	1,497

Nomenclature

A_{IJ} = surface common to Gridblocks I and J
B = FVF
c = constant
f_d = fractional flow
h = net pay thickness
h_{IJ} = grid spacing between Points I and J
$\vec{h}_{IJ}$ = vector pointing from Point I to J
$\underline{k}$ = permeability
$\underline{\underline{k}}$ = permeability tensor
M = mobility ratio
$\vec{n}$ = unity normal vector on Surface A
n_J = number of all neighbors communicating with Gridblock J
n_p = number of all phases
$\bar{p}$ = average pressure of wellblock
p_D = dimensionless pressure
p_{wf} = flowing bottomhole pressure of well
q_{Ik} = production or injection rate
Q_{IJk} = flow through Surface A_{IJ}
r_e = equivalent radius of wellblock
r_w = well radius
S_p = phase saturation
t_{Da} = dimensionless time
Δt = shut-in time
$\vec{u}_p, u_p$ = filtration velocity of Phase p
V = control volume
V_p = pore volume
x_{pk} = mole fraction of Component k in Phase p
γ = angle between A_{IJ} and streamline direction
λ_p = phase mobility
$\Lambda_{pk} = \xi_p x_{pk} \lambda_p$
μ = viscosity
ξ_p = specific mole density of Phase p
ϕ = porosity
Φ_p = phase potential

Subscripts

d = displacing phase
D = dimensionless
I,J,K,L = gridblocks or corresponding gridpoints
k = component index
p = phase index
x,y,z = x, y, and z directions

Acknowledgment

We thank the Austrian Science Foundation, which sponsored this research under its Project Number P6301E.

References

1. von Rosenberg, D.W.: "Local Grid Refinement for Finite-Difference Methods," paper SPE 10974 presented at the 1982 SPE Annual Technical Conference and Exhibition, New Orleans, Sept. 26-29.

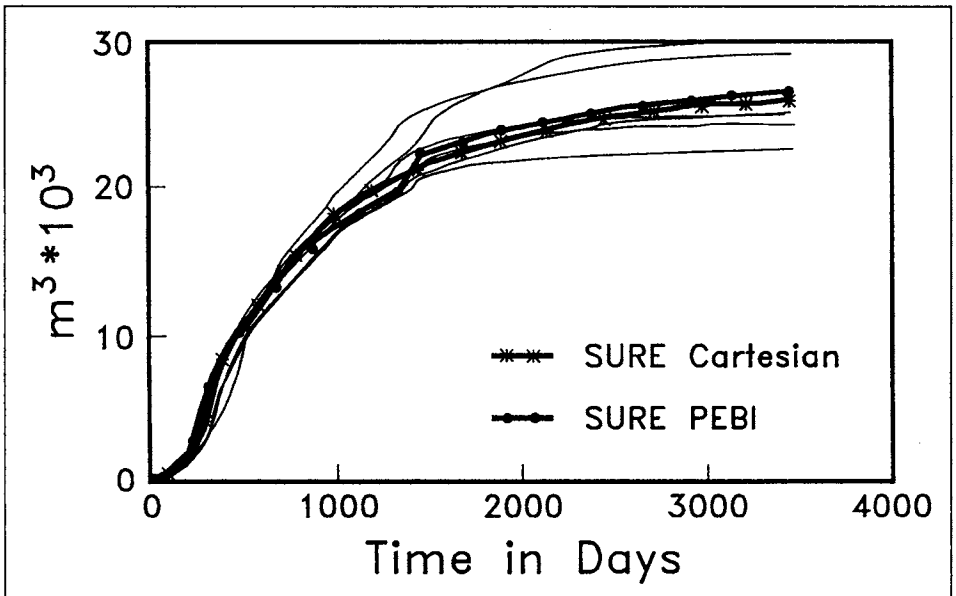

Fig. 14—Cumulative oil production for the full pattern, Fourth SPE Comparative Solution Project.[29]

2. Heinemann, Z., Gerken, G., and Meister, S.: "Anwendung der lokalen Netzverfeinerung bei Lagerstättensimulation," *Erdöl & Erdgas* (June 1983) 199.
3. Heinemann, Z., Gerken, G., and Hantelmann, G.: "Using Grid Refinement in a Multiple-Application Reservoir Simulator," paper SPE 12255 presented at the 1983 SPE Symposium on Reservoir Simulation, San Francisco, Sept. 5–8.
4. Quandalle, P. and Besset, P.: "The Use of Flexible Gridding for Improved Reservoir Modeling," paper SPE 12239 presented at the 1983 SPE Symposium on Reservoir Simulation, San Francisco, Nov. 15–18.
5. Quandalle, P. and Besset, P.: "Reduction of Grid Effects Caused by Local Subgridding in Simulations Using a Composite Grid," paper SPE 13527 presented at the 1985 SPE Symposium on Reservoir Simulation, Dallas, Feb. 10–13.
6. Forsyte, P.A. and Sammon, P.H.: "Local Mesh Refinement and Modeling of Faults and Pinchouts," *SPEFE* (June 1986) 275–85.
7. Yanosik, J.L. and McCracken, T.A.: "A Nine-Point, Finite-Difference Reservoir Simulator for Realistic Prediction of Adverse-Mobility-Ratio Displacements," *SPEJ* (Aug. 1979) 253–62; *Trans.*, AIME, **267.**
8. Coats, K.H. and Modine, A.D.: "A Consistent Method for Calculating Transmissibilities in Nine-Point Difference Equations," paper SPE 12248 presented at the 1983 Symposium on Reservoir Simulation, San Francisco, Nov. 15–18.
9. Pruess, K. and Bodvarsson, G.S.: "A Seven-Point Finite-Difference Method for Improved Grid Orientation Performance in Pattern Steamfloods," paper SPE 12252 presented at the 1983 Symposium on Reservoir Simulation, San Francisco, Nov. 15–18.
10. Hirasaki, G.J. and O'Dell, P.M.: "Representation of Reservoir Geometry for Numerical Simulation," *SPEJ* (Dec. 1970) 393–404; *Trans.*, AIME, **249.**
11. Sonier, F. and Chaumet, P.: "A Fully Implicit Three-Dimensional Model in Curvilinear Coordinates," *SPEJ* (Aug. 1974) 361–70; *Trans.*, AIME, **257.**
12. Robertson, G.E. and Woo, P.T.: "Grid Orientation Effects and the Use of Orthogonal Curvilinear Coordinates in Reservoir Simulation," paper SPE 6100 presented at the 1976 SPE Annual Technical Conference and Exhibition, New Orleans, Oct. 3–6.
13. Fleming, G.C.: "Modeling the Performance of Fractured Wells in Pattern Floods Using Orthogonal, Curvilinear Grids," paper SPE 16973 presented at the 1987 SPE Annual Technical Conference and Exhibition, Dallas, Sept. 27–30.
14. Nghiem, L.X.: "An Integral Approach To Discretizing the Reservoir Flow Equations," *SPERE* (May 1988) 685–90.
15. Pedrosa, O.A. and Aziz, K.: "Use of Hybrid Grid in Reservoir Simulation," *SPERE* (Nov. 1986) 611–21; *Trans.*, AIME, **282.**
16. Pruess, K. and Narasimhan, T.N.: "A Practical Method for Modeling Fluid and Heat Flow in Fractured Porous Media," *SPEJ* (Feb. 1985) 14–26.
17. Rozon, B.J.: "A Generalized Finite-Volume Discretization Method for Reservoir Simulation," paper SPE 18414 presented at the 1989 SPE Symposium on Reservoir Simulation, Houston, Feb. 6–8.
18. Forsyth, P.A.: "A Control-Volume Finite-Element Method for Local Mesh Refinement in Thermal Reservoir Simulation," *SPERE* (Nov. 1990) 561–66; *Trans.*, AIME, **289.**
19. Heinrichs, B.: *Finite-Difference Methods on Irregular Networks*, Birkhäuser, Basel, Boston, Stuttgart (1987).
20. Thompson, J.F., Warsi, Z., and Wayne Mastin, C.: *Numerical Grid Generation*, Elsevier Science Publishing Co. Inc., New York City (1985).
21. Todd, M.R., O'Dell, P.M., and Hirasaki, G.J.: "Methods for Increased Accuracy in Numerical Reservoir Simulators," *SPEJ* (Dec. 1972) 515–30; *Trans.*, AIME, **253.**
22. Holloway, C.C., Thomas, L.K., and Pierson, R.G.: "Reduction of Grid Orientation Effects in Reservoir Simulation," paper SPE 5522 presented at the 1975 SPE Annual Technical Conference and Exhibition, Sept. 28–Oct. 1.
23. Ko, S.C.M. and Au, A.D.K.: "A Weighted Nine-Point Finite-Difference Scheme for Eliminating the Grid Orientation Effect in Numerical Reservoir Simulation," paper SPE 8248 presented at the 1979 SPE Annual Technical Conference and Exhibition, Las Vegas, Sept. 23–26.
24. Frauenthal, J.C., di Franco, R.B., and Towler, B.F.: "Reduction of Grid-Orientation Effects in Reservoir Simulation With Generalized Upstream Weighting," *SPEJ* (Dec. 1985) 902–08.
25. Vinsome, P.K.W. and Au, A.D.K.: "One Approach to the Grid Orientation Problem in Reservoir Simulation," *SPEJ* (April 1981) 160–61.
26. Potempa, T.: "Three-Dimensional Simulation of Steamflooding With Minimal Grid Orientation," paper SPE 11726 presented at the 1983 SPE California Regional Meeting, Ventura, March 23–25.
27. Heinemann, Z.E. and Brand, C.W.: "Gridding Techniques in Reservoir Simulation," *Proc.*, First Intl. Forum on Reservoir Simulation, Alpbach, Austria (Sept. 12–16, 1988).
28. Ramey, H.J. Jr., Kumar, A., and Gulati, M.S.: *Gas Well Test Analysis Under Water-Drive Conditions*, American Gas Assn., Arlington, VA (1973).
29. Aziz, K., Ramesh, B., and Woo, P.T.: "Fourth SPE Comparative Solution Project: Comparison of Steam Injector Simulators," *JPT* (Dec. 1987) 1576–84.

Appendix—Anisotropic Permeability Tensor

Derivation of $\nabla\Phi$. Let I, J, K, and L be four points not in a common plane. Let $\Phi_I \ldots \Phi_L$ denote the values of the potential in these points. Assume that $\Phi(x)$ is defined by linear interpolation within the tetrahedron spanned by these points (cf. Fig. 1). This is the most simple assumption. Of course, by taking into account more gridpoints, we can obtain better approximations. Physical concepts, as well, can suggest another function to fit the potential. In a problem with nearly radial flow, an approximation that is linear in the logarithm can be more appropriate.

The potential gradient within this element is then given by

$$\nabla\Phi = \begin{bmatrix} h_{11} & h_{12} & h_{13} \\ h_{21} & h_{22} & h_{23} \\ h_{31} & h_{32} & h_{33} \end{bmatrix}^{-1} \begin{bmatrix} \Phi_J - \Phi_I \\ \Phi_K - \Phi_I \\ \Phi_L - \Phi_I \end{bmatrix} = \mathbf{A}^{-1}\delta\vec{\Phi}. \quad \ldots (A\text{-}1)$$

Here, the rows of Matrix A contain the row vectors $\vec{h}_{IJ}$, $\vec{h}_{IK}$, and $\vec{h}_{IL}$, pointing from Gridpoint I to Gridpoints J, K, and L, respectively. In $\delta\vec{\Phi}$, the potential differences are arranged as a (column) vector. It follows for the scalar product $\nabla\Phi \cdot \vec{n}$, that

$$k\nabla\Phi \cdot \vec{n} = k\vec{a} \cdot \delta\vec{\Phi} = k[a_1(\Phi_J - \Phi_I) + a_2(\Phi_K - \Phi_I) + a_3(\Phi_L - \Phi_I)], \quad \ldots (A\text{-}2)$$

where $\vec{a} = (a_1, a_2, a_3)$ is given as the solution of the system

$$\mathbf{A}^T\vec{a} = \vec{n}, \quad \vec{a} = (A^T)^{-1}\vec{n}. \quad \ldots (A\text{-}3)$$

$\mathbf{A}^T$ = transpose of A; i.e., the matrix containing $\vec{h}_1$, $\vec{h}_2$, and $\vec{h}_3$ written as column vectors.

In many cases, a scalar permeability cannot model the flow behavior in a porous medium and a tensor quantity, $\bar{\bar{k}}$, is used. In a finite-difference approach, one has to approximate terms like

$$\nabla \cdot (\bar{\bar{k}}\nabla\Phi) = k_{11}\Phi_{xx} + k_{22}\Phi_{yy} + k_{33}\Phi_{zz} + 2k_{12}\Phi_{xy} + 2k_{13}\Phi_{xz} + 2k_{23}\Phi_{yz}. \quad \ldots (A\text{-}4)$$

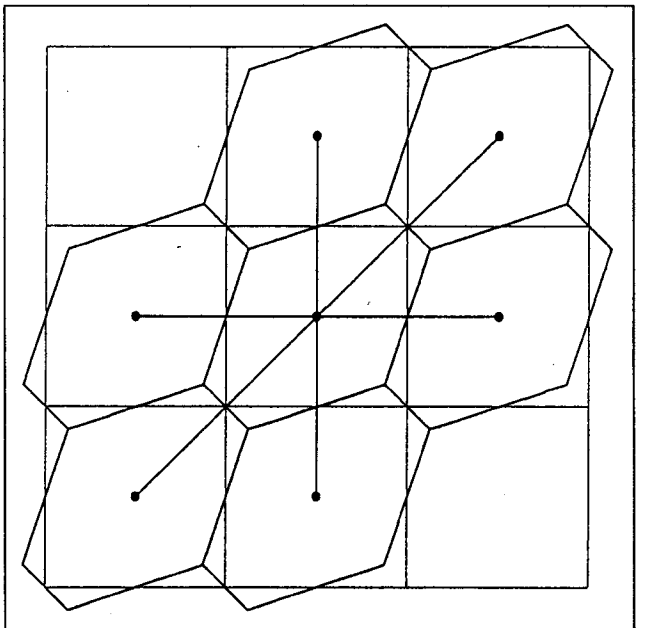

Fig. A-1—$\bar{\bar{k}}$-orthogonal block system. $\bar{\bar{k}} = \begin{bmatrix} 3 & 1 \\ 1 & 3 \end{bmatrix}$.

Authors

Brand

Munka

Chen

Heinemann

Zoltan E. Heinemann is professor and head of the Dept. of Reservoir Engineering at the Mining U. Leoben in Austria. He holds a PhD degree in reservoir engineering and an MS degree in petroleum engineering from the U. for Heavy Industries in Miskolc, Hungary, and a degree in petroleum engineering from the Ecole Natl. Supérieure du Pétrole et des Moteurs in Paris. He is involved with reservoir engineering, reservoir simulation, and EOR and is an experienced consultant and lecturer. He is the author of more than 50 papers and several textbooks. Clemens W. Brand is a research scientist in the Reservoir Engineering Dept. at the Mining U. Leoben. His research responsibilities include numerical grid generation, discretization methods, and linear solvers. He holds MS and PhD degrees from the U. of Vienna. Margit Munka is a reservoir engineer for Heinemann Oil Technology in Austria. She holds BS, MS, and PhD degrees in petroleum engineering from the U. of Heavy Industries in Miskolc, Hungary. She previously worked for 5 years in the Research Laboratory for Mining Chemistry of the Hungarian Academy of Sciences. Youming Chen holds BS and MS degrees in petroleum geology from the Chengdu C. of Geology in China and a PhD degree in reservoir engineering from the Mining U. Leoben, where he has been studying reservoir engineering since 1985.

On a Cartesian grid, the mixed derivative terms cannot be approximated by the usual five-point (in 2D) or seven-point (in 3D) discretization formulas. In a finite-volume approach, when all components of $\nabla\Phi$ are evaluated, the product $\bar{\bar{k}}\nabla\Phi$ can be computed by a matrix-vector multiplication. Thus, the implementation of a tensor permeability does not cause fundamental difficulties. But under certain assumptions analogous to the case of scalar k, the computation can be simplified.

Case 1. Block surfaces are oriented perpendicular to the principal axes of $\bar{\bar{k}}$ and perpendicular to the straight lines connecting neighboring gridpoints. This is the case if a Cartesian grid is oriented corresponding to the principal axes of $\bar{\bar{k}}$ (which then is transformed to diagonal form). Eq. 6 is valid. For k, one has to use one of the principal values of $\bar{\bar{k}}$, depending on the orientation of A_{IJ}.

Case 2. In the streamtube case, the effects of anisotropy are already taken into account during the proper calculation of streamlines. When Points I and J lie in the same streamtube, the vector $\bar{\bar{k}}\nabla\Phi$ is parallel to $\vec{h}_{IJ}$. Let γ denote the angle between A_{IJ} and the streamline direction. Then,

$$(\bar{\bar{k}}\nabla\Phi)\cdot\vec{n}=(\Phi_J-\Phi_I)\frac{|h_{IJ}|}{(\bar{\bar{k}}^{-1}\vec{h}_{IJ})\cdot\vec{h}_{IJ}}\cos\gamma. \quad \ldots\ldots\ldots\ldots (A\text{-}5)$$

Case 3. The $\bar{\bar{k}}$-orthogonal grid. This is a generalization of the perpendicular bisection grid. The surface A_{IJ} is oriented so that $\bar{\bar{k}}\vec{n}$ is parallel to $\vec{h}_{IJ}$. An example of a $\bar{\bar{k}}$-orthogonal grid is shown in **Fig. A-1.** In this case,

$$(\bar{\bar{k}}\nabla\Phi)\cdot\vec{n}=\frac{|\bar{\bar{k}}\vec{n}|}{h_{IJ}}(\Phi_J-\Phi_I). \quad \ldots\ldots\ldots\ldots\ldots\ldots\ldots (A\text{-}6)$$

SI Metric Conversion Factors

bbl × 1.589 873 E−01 = m^3
ft^3 × 2.831 685 E−02 = m^3

SPERE

Original SPE manuscript received for review Feb. 6, 1988. Paper accepted for publication March 20, 1990. Revised manuscript received Feb. 21, 1990. Paper (SPE 18412) first presented at the 1989 SPE Symposium on Reservoir Simulation held in Houston, Feb. 6–8.